Theoretical and Computational Acoustics
D. Lee, Y-H Pao, M.H. Schultz, and Y-C Teng (Editors)

Using Matched Field Processing to Determine Shallow Water Environmental Parameters

A. Tolstoy
Integrated Performance Decisions, 4224 Waialae Avenue, Suite 5-260,
Honolulu HI 96816

The indirect estimation of environmental parameters is notoriously difficult. A new approach involves Matched Field Processing (a signal processing technique applied to acoustic array data) which in combination with careful experimental design has the potential to estimate such properties as sound-speed profiles (in the water and in the bottom), layer thicknesses and densities, number of layers, etc. In particular, the technique may be capable of estimating those environmental parameters to which the acoustic field is most sensitive. However, each environmental situation requires careful design. Issues which need to be resolved for a given scenario include: what are the optimal frequencies for processing, what are the optimal array and source configurations, what properties affect the acoustic fields and what are their associated sensitivities. Most importantly, we are finding that critical components of the overall problem are: (1) the optimization process which must search through tens of thousands of parameter combinations to find the "best" match; (2) the potential non-uniqueness of the "best" match, i.e., there seem to be families of solutions which provide comparable optimizing fits to data. Present efforts are focused on these questions as applied to simulated and experimental data.

1. Introduction

Shallow water scenarios presently provide an important focus for much underwater acoustic research. As a consequence there is now a desperate need for accurate and fast propagation models to describe acoustic behavior in difficult-to-model, complicated shallow water conditions. Factors such as sediment thicknesses and sound-speeds have become critical model inputs but are nearly impossible to obtain by direct measurements, particularly in highly variable regions where many samples are needed. Thus, intense efforts are being made to develop indirect, remote sensing techniques which involve the solution of inverse problems, i.e., problems for which one must infer the unknown model input parameters from the observed model output.

Many inverse techniques to determine bottom properties are currently being pursued (see Frisk [1990]), and the newest involve the use of Matched Field Processing (MFP) which involves both the amplitude and phase of a signal measured along an array of receivers (see Tolstoy [1993] for general details on MFP). The MFP techniques often involve simple least squares fits of model predictions to data and which are subsequently combined with computationally intense, random number based methods such as simulated annealing (Lindsay and Chapman [1993]; Dosso et al. [1993]; Collins et al. [1992]; Collins and Kuperman [1991]) and/or genetic algorithms (Gingras and Gerstoft [1995]; Gerstoft [1994a,b, 1995]).

The approach to be discussed in this paper is not a least squares fit nor is it random-number based. It is based on the high resolution non-linear minimum-variance (MV) processor plus a global, directed search through parameter space. The MV processor was selected primarily because the standard Linear Processor does not show sufficient sensitivity to the parameters.

2. The Test Case: Experimental Data

In this paper we will analyze a simple scenario: no range or azimuthal variability, a single source, a single vertical array where we will subsequently estimate shallow water bottom parameters for *experimental* test data. We shall use the KRAKEN normal mode model (Jensen et al. [1994]) as our propagation component.

Consider a shallow water environment consisting of a thin sediment layer (thickness h_{sed}) with a linear sound-speed profile (varying from c_1 at the top of the sediment layer to c_2 at the bottom of the sediment layer) with constant density ρ_1 and which overlays another sediment layer (thickness 100m) with linear sound-speed profile (varying from $c_{1,bot}$ at the top to $c_{2,bot}$ at the bottom of the layer) with constant density ρ_2. These two layers overlay a non-elastic half space with a constant sound-speed $c_{2,bot}$ and density ρ_2. Nominal bottom parameter values are as indicated in Fig. 1 and Table 1 (such values were suggested in Jensen [1974]).

parameter	value
h_{sed}	3.5m
h_{water}	114m
$c_{1,bot}$	1600m/s
$c_{2,bot}$	1600m/s
c_1	1490m/s
c_2	1490m/s
r_{sou}	12.1km
z_{sou}	20m
ρ_1	1.5
ρ_2	1.8
Δz_{arr}	0.0m

Table 1. Nominal parameter values.

This scenario corresponds to a subset of Mediterranean Sea experimental test data collected in October 1993 where the measured water column sound-speed profile resulted in downward refracting energy. For this sea test a 64m array (with a data sampling rate of 1000 per s, a window of 60 to 420Hz) was deployed and moored to the bottom with nominal coordinates determined by GPS positioning while a second ship deployed 25 shots over the side at various ranges. The full array consisted of 64 phones at non-uniform intervals from

35.72m depth to 99.72m. We will begin processing with the 100.6Hz component of the signal (composed of approximately 5 propagating modes for the nominal parameter values) and will only consider a subarray of data consisting of 9 phones at 8m intervals (approximately half-wavelength intervals at 100Hz). We note that if a non-uniformly spaced array were to be used, the results would be biased toward those parameters most strongly affecting the field measured on the most densely packed phones. In the results to follow we examine only a single shot corresponding to a source at a nominal range of 12.1km (uncertain to within ±200m), depth of 20m (uncertain to within ±10m) and will be using 1.024s of those data.

First, we assume the nominal parameter values and subsequently compare the model predictions for a variety of source ranges and depths with the measured data. The result is shown in Fig. 2 as an ambiguity surface (AMS) for the MV processor where we find that the best correlation between data and model occurs for a source predicted to be at 12.66km, 30.0m. This position is not "properly" located (it should be within the range and depth limits indicated by the error bars centered on the nominal position of 12.1km, 20m). Moreover, the peak value of 0.048 out of a maximum value of 1.00 is not very encouraging. Clearly, there is a significant mismatch between model predictions and the measured data.

parameter	interval	increment	no. of values
h_{sed}	[0.5,9.5] (m)	0.25m	37
h_{water}	[110,120] (m)	0.25m	41
$c_{1,bot}$	[1550,1650] (m/s)	2.0m/s	51
$c_{2,bot}$	[1550,1680] (m/s)	5.0m/s	27
c_1	[1450,1650] (m/s)	5.0m/s	41
c_2	[1450,1650] (m/s)	5.0m/s	41
r_{sou}	[11.9,12.3] (km)	0.05km	9
z_{sou}	[10,30] (m)	5m	5
ρ_1	[1.0,2.0]	0.1	11
ρ_2	[1.0,2.5]	0.1	16
Δz_{arr}	[-3.5,3.5] (m)	0.5	15

Table 2. Initial parameter search values, their search intervals, increments, and number of candidates.

Recent work has resulted in much improved predictions after searching the parameter space shown in Table 2 where we also include a possible array shift in depth Δz_{arr}. In particular, we have found that values shown in Table 3 result in the AMS shown in Fig. 2 where the source is now well located near the nominal/measured position and the peak value is 0.48.

At this point we ask a number of important questions:

1. How nasty is the parameter space through which we have been searching?

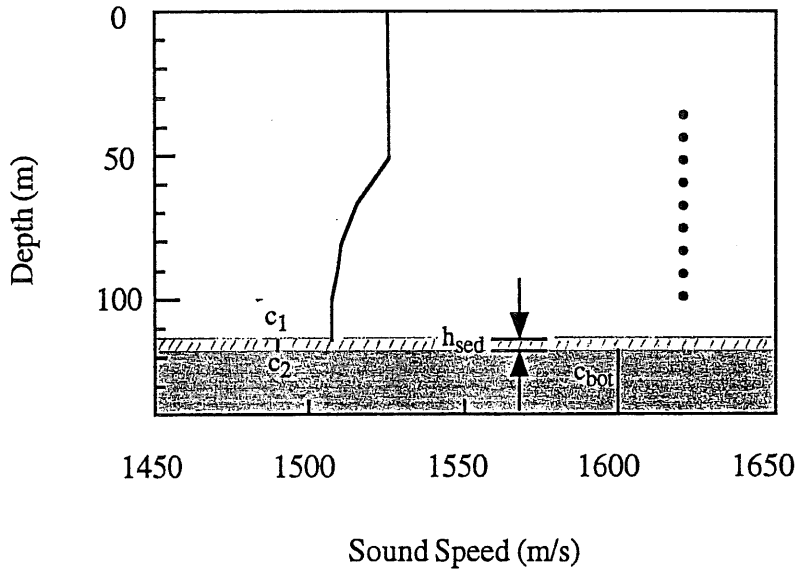

Figure 1: Nominal geoacoustic parameters and uniform subarray parameters for a shallow water test case in the Mediterranean north of Elba.

2. What can we do to improve our search, e.g., to flatten out troublesome sidelobes?

3. How accurate is our "solution"? That is, how much do we trust our final solution relative to the physical reality? Is our "solution" unique?

4. When do we stop looking for a better solution?

To address these questions, we shall now examine simulated data over which we have total control and knowledge.

3. The Test Case: Simulated Data

Let us consider "data" generated by the KRAKEN model at 100.6Hz using the improved parameters of Table 3. In Fig. 4 we see an AMS showing the MV processor sensitivity to param1=$c_{1,bot}$ (varying only from 1590m/s to 1620m/s) and param2=h_{sed} (varying from 0.5m to 9.5m). The peak=1.00 occurs at the true values $c_{1,bot}$=1601m/s, h_{sed}=2.6m with the other parameters fixed at their true values. We note that the AMS shows many ripples and local maxima, i.e., sidelobes. While these sidelobes are not major peaks, they will increase the computational difficulty in finding the true global maximum. In an effort to smooth out these ripples let us consider a broadband approach. In particular, let us first

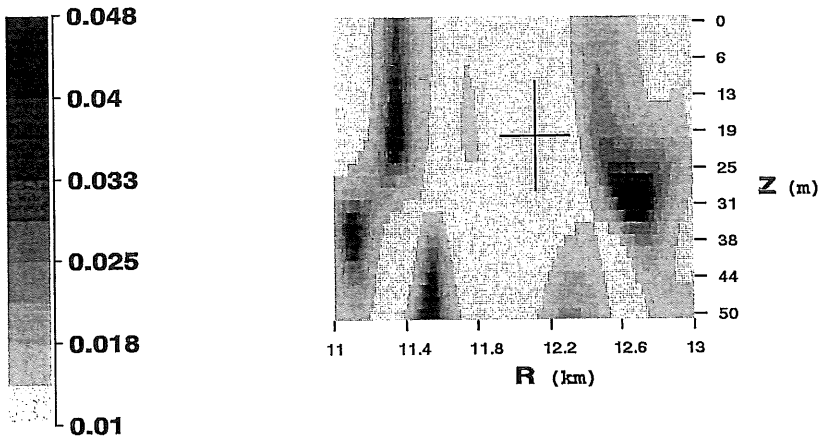

Figure 2: AMS for test data at 100.6Hz using nominal geoacoustic parameters. Source is mislocated at 12.66km, 30.0m, off from nominal values of 12.1±0.2km, 20±10m with peak value of 0.048.

look at the AMSs for a selection of frequencies: 75.6Hz, 125.6Hz and 150.6Hz as seen in Figs. 5a,b,c. We note that at the higher frequencies we have more ripples although they are generally with lower peak values. Moreover, the global maximum is narrower in width. If we add the four frequencies (75.6, 100.6, 125.6, 150.6Hz) we arrive at Fig. 5d where the sidelobes are down from the single 100.6Hz AMS. However, the remaining global maximum will be hard to find since it is now narrower and surrounded by more ripples. In general we find that merely increasing frequency may make the optimization problem harder. This suggests a closer look at the lower frequencies.

In Fig.6 we show AMSs for 50.6Hz, 55.6Hz, and a sum over six frequencies (50.6, 55.6 60.6, 65.6, 70.6, 75.6Hz). We see that the final sum is an improvement over the individual components including those at 75.6Hz (Fig. 5a) and at 100.6Hz (Fig. 4). This suggests that lower frequencies may be optimal for a broadband approach and that this broadband approach may result in improved optimization searches.

The next major issue becomes: how accurate and trustworthy is a "solution". While searching through the parameter space a number of major sidelobes turned up, i.e., combinations of parameter values which produce nearly *identical* acoustic fields to that of the simulated data. As an example, consider the values shown in Table 4. In Fig. 7 we see AMSs at various frequencies assuming the "data" field generated by parameters shown in Table 3 but the model fields generated using the sidelobe parameter values listed in Table 4 except for $c_{1,bot}, h_{sed}$ which are varied. We see that the sidelobe remains strong with a peak=0.95 or better at multiple frequencies and for the broadband AMS (summing over

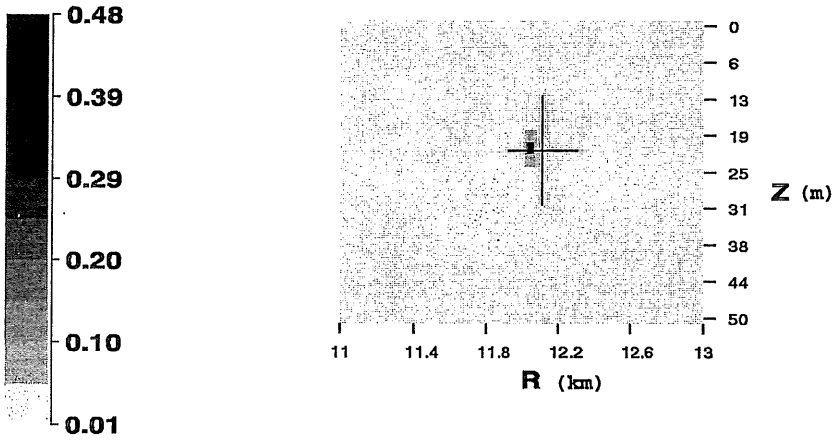

Figure 3: AMS for test data at 100.6Hz using improved geoacoustic parameters. Source is correctly located at 12.05km, 20.0m with peak value of 0.48.

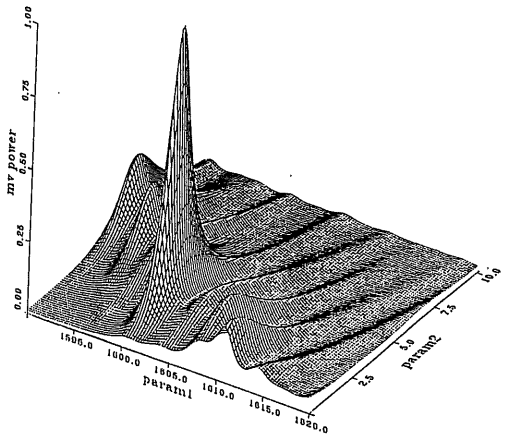

Figure 4: AMS at 100.6Hz simulated data for param1=$c_{1,bot}$, param2=h_{sed} with other parameters fixed at their true values as given in Table 3.

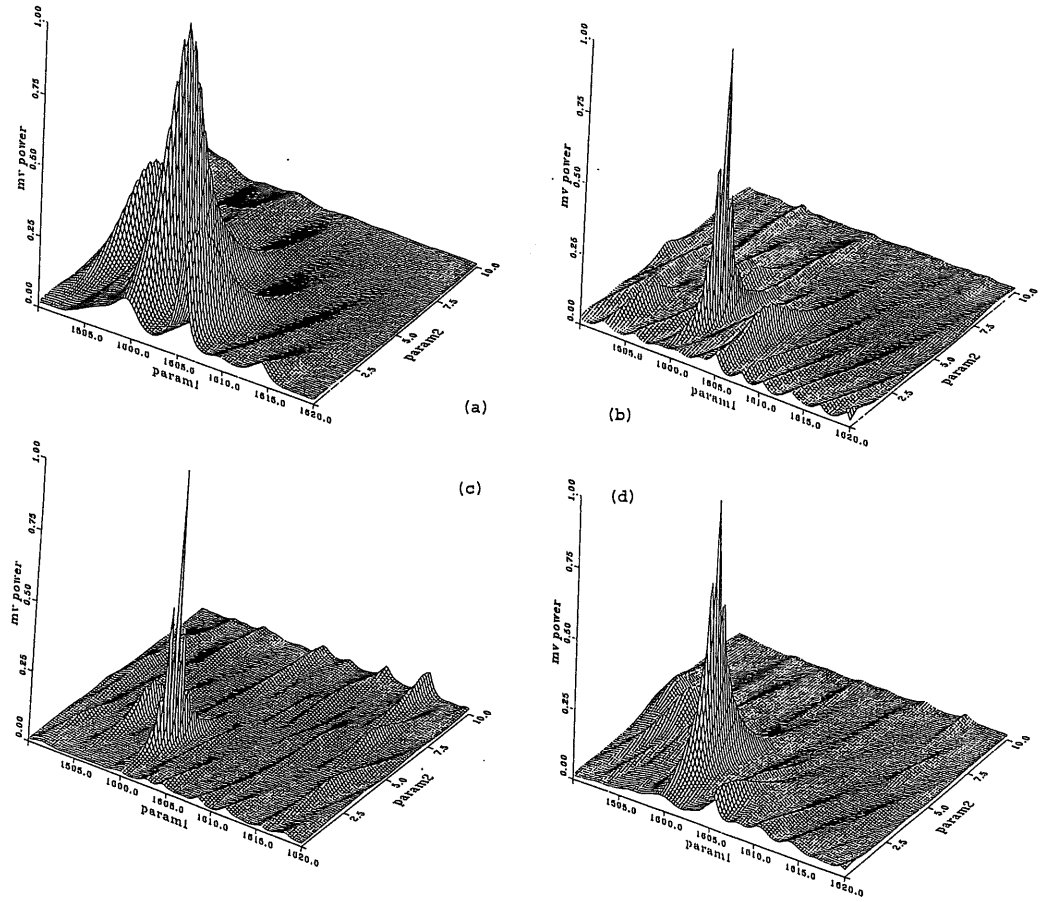

Figure 5: AMSs at a variety of frequencies for simulated data for param1=$c_{1,bot}$, param2=h_{sed} with other parameters fixed at their true values as given in Table 3. (a) 75.6Hz; (b) 125.6Hz; (c) 150.6Hz; (d) sum over 75.6, 100.6, 125.6, and 150.6Hz.

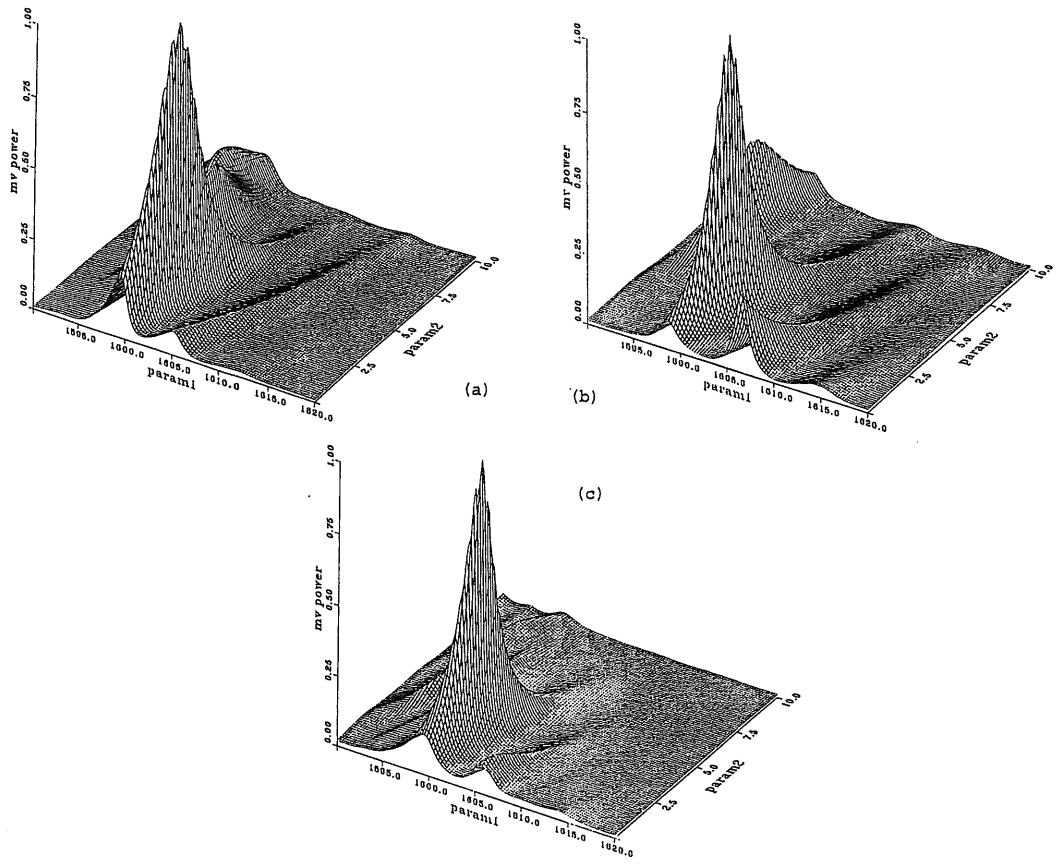

Figure 6: AMSs at a variety of lower frequencies for simulated data for param1=$c_{1,bot}$, param2=h_{sed} with other parameters fixed at their true values as given in Table 3. (a) 50.6Hz; (b) 55.6Hz; (c) sum over 50.6, 55.6, 60.6, 65.6, 70.6, 75.6Hz.

Figs. 7a,b,c as shown in Fig. 7d). Thus, even a broadband approach may not eliminate some false solutions.

parameter	value
h_{sed}	2.6m
h_{water}	115.5m
$c_{1,bot}$	1601m/s
$c_{2,bot}$	1691m/s
c_1	1620m/s
c_2	1662m/s
r_{sou}	12.05km
z_{sou}	20m
ρ_1	1.15
ρ_2	1.35
Δz_{arr}	-3.4m

Table 3. Improved parameter values.

Finally, in an effort to tamp down this sidelobe we consider a number of source ranges. In particular, consider AMSs at 100.6Hz shown in Fig.8 for a source at ranges 8.05km, 10.05km, 12.05km (Fig. 7c), and 14.05km. Each of these AMSs shows very strong peaks from 0.88 to 0.95. However, the peaks occur at slightly different parameter values. Then, adding the surfaces together results in Fig. 8d with a peak value of 0.75. Thus, we conclude that sources at different ranges sense the bottom differently with the result that sidelobes will be different for different ranges. Therefore, a variety of source positions may help to eliminate false solutions. Unfortunately, this variation will not help in a range-varying environment.

4. Conclusions

We conclude that Matched Field Processing can be an important tool for the estimation of shallow water bottom properties. We have examined experimental data and found significant improvement in matching the measured field with the modeled field for a number of parameter value combinations. We have also investigated a number of issues by means of simulated data and find that:

- Broadband processing with an emphasis on the *lower* frequencies can help to flatten out the parameter search space while retaining a broad main peak resulting in more efficient search schemes.

- A variety of source ranges can also flatten out sidelobes in the search space reducing false peaks which can appear across frequencies.

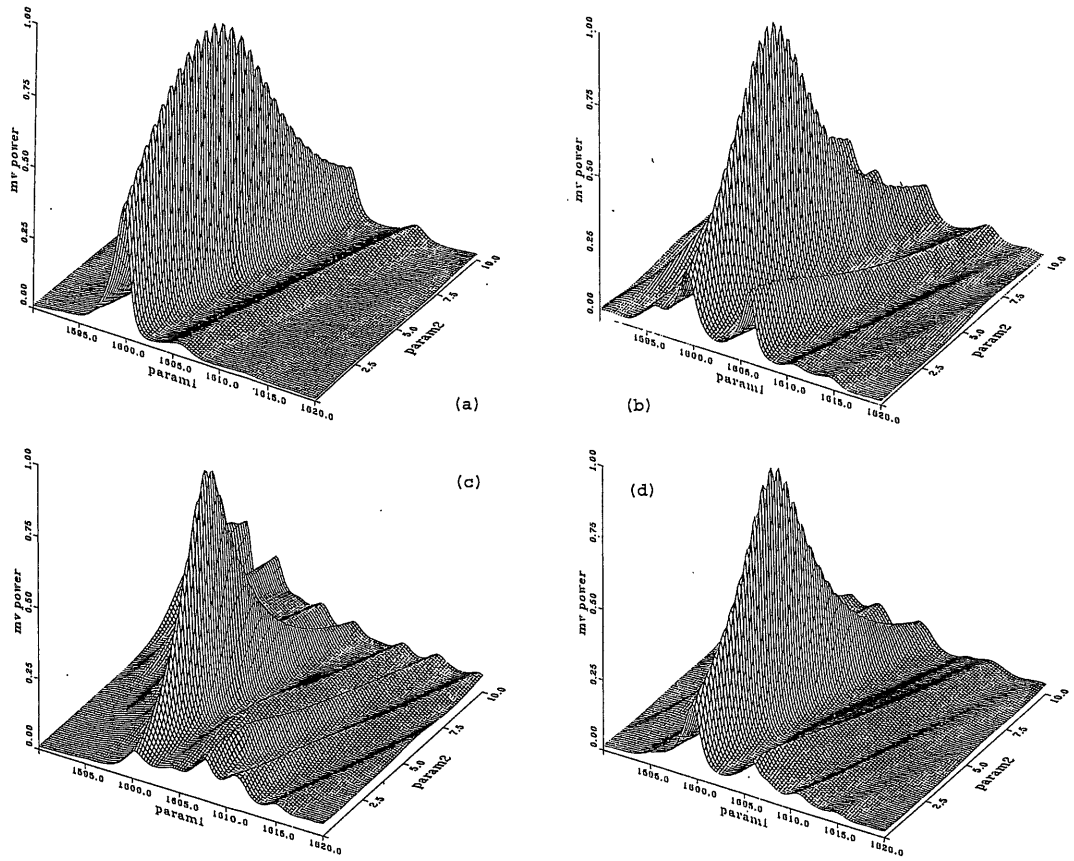

Figure 7: AMSs at a variety of frequencies for simulated data (with true values of Table 3) varying param1=$c_{1,bot}$, param2=h_{sed} with other parameters fixed at the sidelobe values as given in Table 4. (a) 50.6Hz; (b) 75.6Hz; (c) 100.6Hz; (d) sum over 50.6, 75.6, and 100.6Hz. We notice that the peak has not significantly decreased as a consequence of the summation and is still high at 0.96.

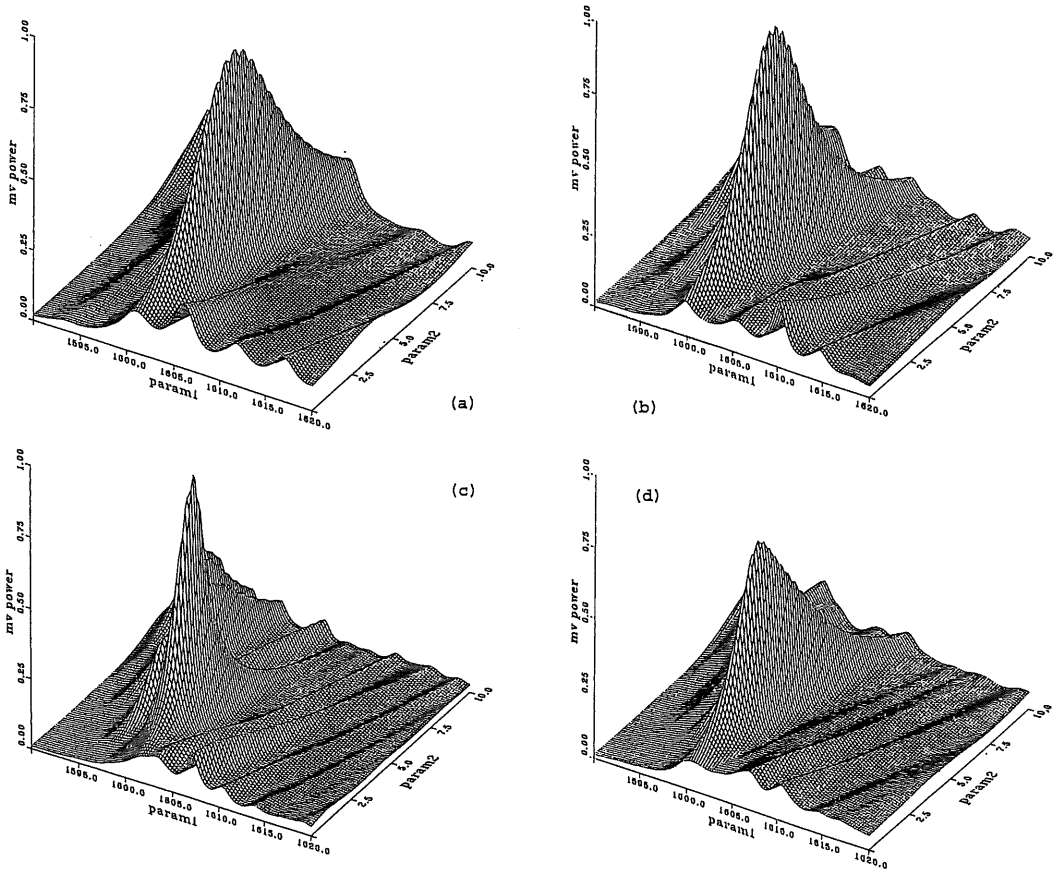

Figure 8: AMSs at a variety of source ranges for simulated data (generated using values of Table 3) varying param1=$c_{1,bot}$, param2=h_{sed} with other model parameters fixed at the sidelobe values as given in Table 4. (a) 8.05km; (b) 10.05km; (c) 14.05km; (d) sum over 8.05, 10.05, 12.05, 14.05km. We note how the peak has decreased from a value near 0.95 to 0.75.

However, difficulties still remain, and these difficulties cut across all inversion techniques. In particular,

- The search for one optimizing solution is extremely difficult. It is complicated by the facts that the parameter space is enormous and the response surface is highly non-convex.
- There is no satisfactory way to determine when the "best" solution has been found. Peak responses will always be less than the ideal value of 1.00. When are these lower values the result of not having located a better combination of parameters versus the result of mismatch in the assumed model of the scenario?

Finally, the issue of non-uniqueness is critical. All the inversion techniques developed to address shallow water environmental properties are plagued by sidelobes of one kind or another. It is not clear at this point how the various techniques compare: time domain versus frequency domain? vertical versus horizontal samplings? Phase only versus full field? This may be a good time to investigate the variety of presently existing inversion techniques as applied to some uniform, simulated data sets. Some methods may offer advantages over others, particularly under certain conditions.

parameter	value	error
h_{sed}	3.3m	+0.7m
h_{water}	115.0m	-0.5m
$c_{1,bot}$	1602m/s	+1m/s
$c_{2,bot}$	1692m/s	+1m/s
c_1	1620m/s	
c_2	1620m/s	-42m/s
r_{sou}	12.05km	
z_{sou}	20m	
ρ_1	1.20	+0.05
ρ_2	1.35	
Δz_{arr}	-3.5m	-0.1m

Table 4. Parameter values for a sidelobe.

5. Acknowledgements

Many thanks to: ONR for funding support, J. Wolf and G. Vermillion of NRL (for the test data: experimental design, data gathering, and data processing), and D. Gingras of SACLANT Centre (as chief scientist on the test cruise and general contributor).

References

1. M.D. Collins and W.A. Kuperman, "Focalization: environmental focusing and source localization", *J. Acoust. Soc. Am.*, **90**, (1991) 1410-1422.
2. M.D. Collins, W.A. Kuperman, and H. Schmidt, "Nonlinear inversion for ocean-bottom properties", *J. Acoust. Soc. Am.*, **92**, (1992) 2770-2783.
3. S.E. Dosso, M.L. Yeremy, J.M. Ozard, and N.R. Chapman, "Estimation of ocean-bottom properties by matched field inversion of acoustic field data", *IEEE J. Oceanic Eng.*, **18**, (1993) 232-239.
4. G.V. Frisk, "Inverse methods in ocean bottom acoustics", in *Les Houches Session L Oceanographic and Geophysical Tomography* (North-Holland, Amsterdam. 1990).
5. P. Gerstoft, "Inversion of seismoacoustic data using genetic algorithms and *a posteriori* probability distributions", *J. Acoust. Soc. Am.*, **95**, (1994a) 770-782.
6. P. Gerstoft, "Global inversion by genetic algorithms for both source position and environmental parameters", *J. Computat. Acoust.*, **3**, (1994b) 251-266.
7. P. Gerstoft, "Inversion of acoustic data using a combination of genetic algorithms and the Gauss-Newton approach", *J. Acoust. Soc. Am.*, **97**, (1995) 2181-2190.
8. D.F. Gingras and P. Gerstoft, "Inversion for geometric and geoacoustic parameters in shallow water: Experimental results", *J. Acoust. Soc. Am.*, **97**, (1995) 3589-3598.
9. F.B. Jensen, "Comparision of transmission loss data for different shallow-water areas with theoretical results provided by a three-fluid normal-mode propagation model", in *SACLANTCEN Conf. Proc.* No. 14 (1974).
10. F.B. Jensen, W.A. Kuperman, M.B. Porter, and H. Schmidt, *Computational Ocean Acoustics* (Am. Inst. Physics, New York, 1994).
11. C. E. Lindsay, and N.R. Chapman, "Matched field inversion for geoacoustic model parameters using adaptive simulated annealing", *IEEE J. Oceanic Eng.*, **18**, (1993) 224-231.
12. A. Tolstoy, *Matched Field Processing for Underwater Acoustics* (World Scientific Pub, Singapore, 1993).